Energy Loss from Off-shell Quark in Gluon Fields

*Based on: **T. Lappi & IS** arXiv:2607.XXXX*

Ismail Soudi

isma@physik.uni-bielefeld.de

Bielefeld University

Jets in heavy ion collisions

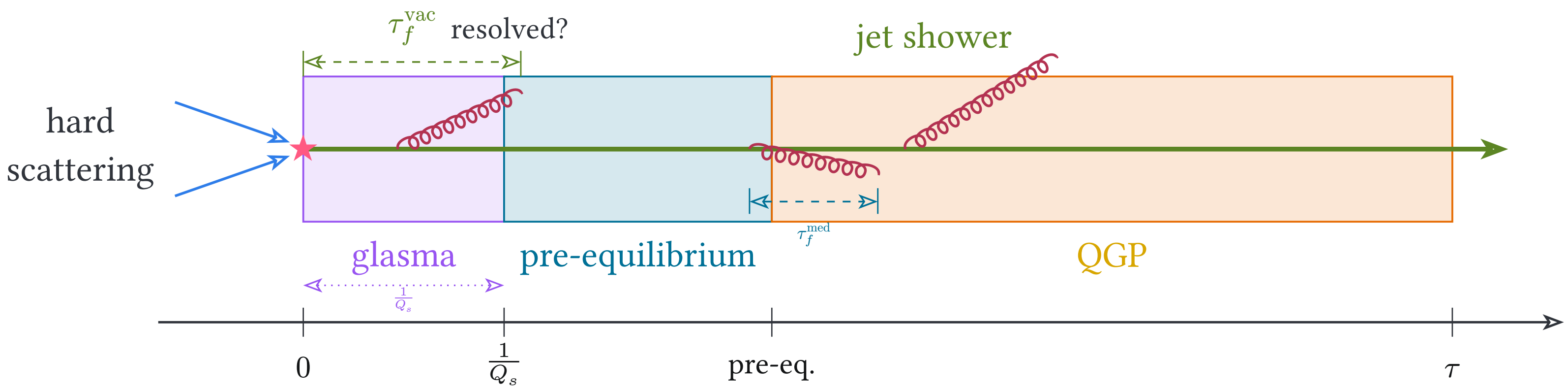

Medium

1. Initial Glasma Fields
2. Out-of-equilibrium evolution
2. Hydrodynamical QGP

Jet

1. Hard production $\tau_{\text{hard}} \sim 1/p_T$
2. Vacuum-like shower
3. Jet-medium Shower

HIC vs Small Systems

Heavy-ion collisions

- Strong signals of collectivity
- Clear quenching observed
- QGP energy loss dominates

Small systems

- Collective-like signals
- No clear jet-quenching signal
- Hard-soft correlations

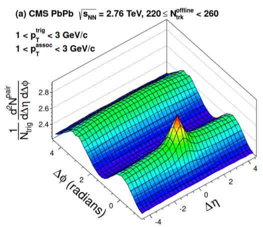

PbPb

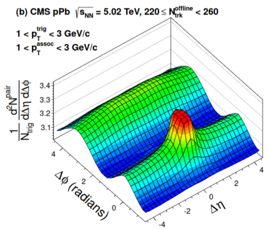

pPb

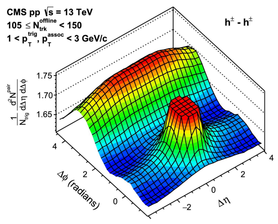

high-mult. pp

System size

- Energy loss v.s. system size
- Early-time v.s. late-time energy loss

[Chatrchyan & others Phys. Lett. B 718, 795–814 2013; Chatrchyan & others Phys. Lett. B 724, 213–240 2013; Khachatryan & others Phys. Lett. B 765, 193–220 2017; Hayrapetyan & others Phys. Rev. Lett. 136, 162301 2026]

HIC vs Small Systems

Heavy-ion collisi ... **systems**

- Strong signals of colle ... ike signals
- Clear quenching obse ... -quenching signal
- QGP energy loss dom ... orrelations

PbPb

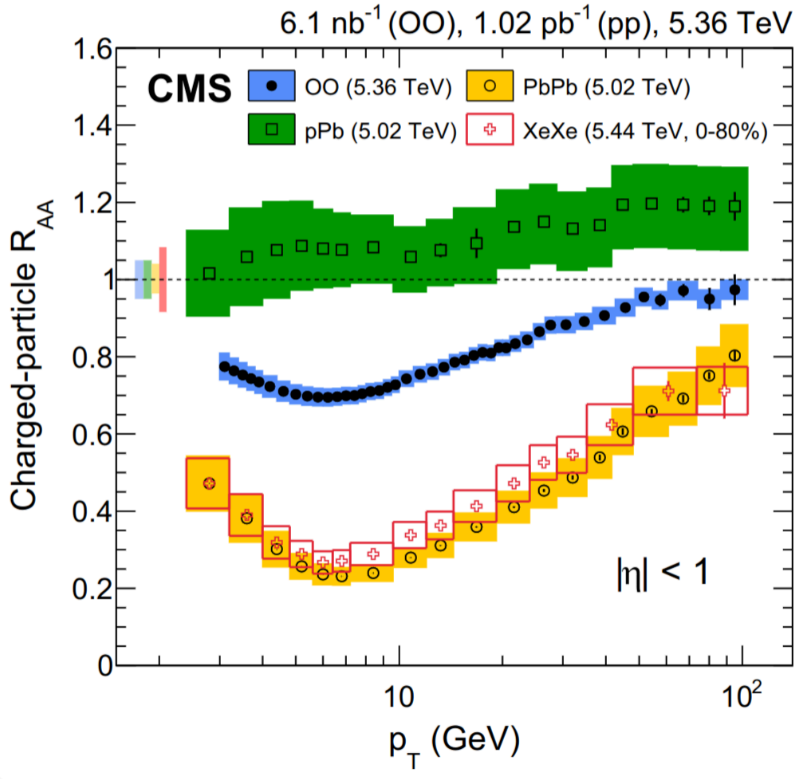

high-mult. pp

- Energy loss v.s. syst ... s. late-time energy loss

[Chatrchyan & others Phys. Lett. B 718, 795–814 2013; Chatrchyan & others Phys. Lett. B 724, 213–240 2013; Khachatryan & others Phys. Lett. B 765, 193–220 2017; Hayrapetyan & others Phys. Rev. Lett. 136, 162301 2026]

Momentum Broadening in Glasma

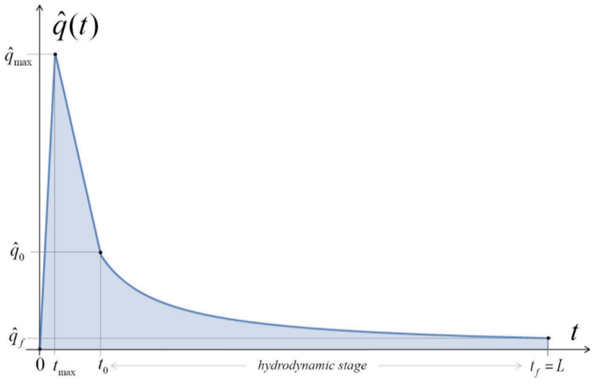

Figure 3: Schematic temporal evolution of $\hat{q}(t)$.

[Carrington et al. Phys. Lett. B 834, 137464 2022]

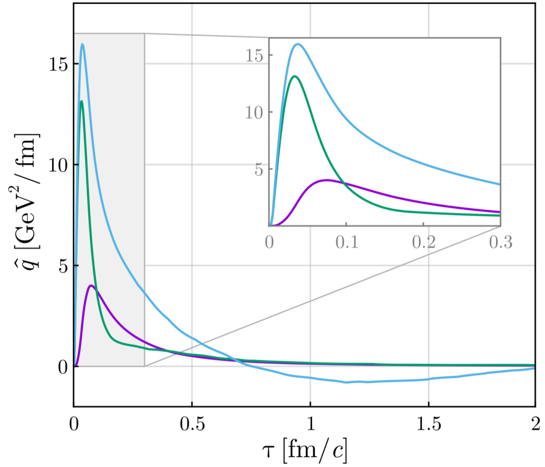

[Avramescu et al. Phys. Rev. D 107, 114021 2023]

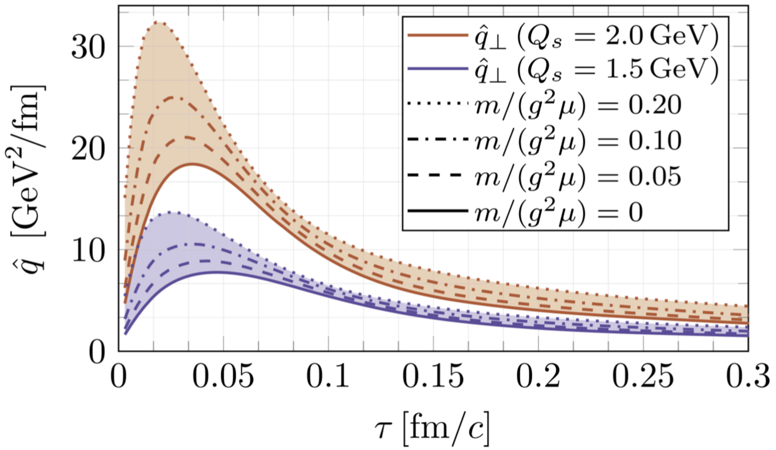

[Ipp et al. Phys. Lett. B 810, 135810 2020]

- Large broadening $\hat{q}_{\text{glasma}} \gg \hat{q}_{\text{QGP}}$
- Short lifetime
- BDMPS-Z Energy loss: $\Delta E \sim \hat{q} L^2$ [Baier et al. Nucl. Phys. B 483, 291–320 1997]

Medium-Induced Radiation

Standard picture

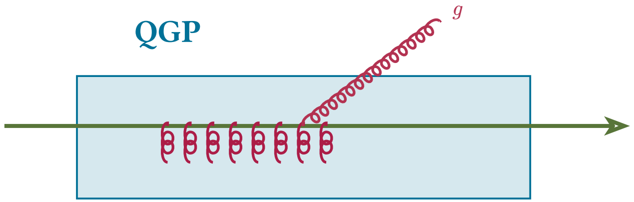

- Medium length $L \gg \tau_{\text{form}}$
- Multiple scatterings (LPM)
- Vacuum/medium separation

  $\longrightarrow$ Jet resolved as on-shell

Early-time Plasma

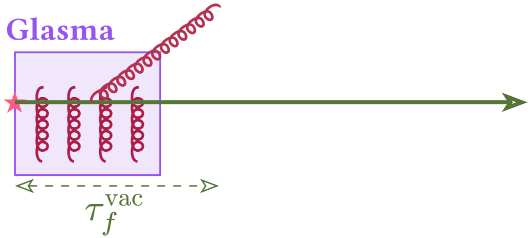

- Short-lived glasma fields
- Highly virtual jet
- Vacuum-like splittings

  $\longrightarrow$ Virtuality vs glasma resolution

First emission: vacuum-like vs glasma modification $\tau_f^{\text{vac}} \Leftrightarrow 1/Q_s.$

Shockwave Framework

- Dense small-x gluons
  - $\longrightarrow$ Classical color field A^μ.
- Fast target is a thin sheet in x^+.
  - $\longrightarrow$ $A^\mu(x) = \delta^{\mu -}\delta(x^+)\alpha(\boldsymbol{x})$.
- Crossing the sheet described by
  - $\longrightarrow$ Wilson line $\mathcal{U}(\boldsymbol{x})$.

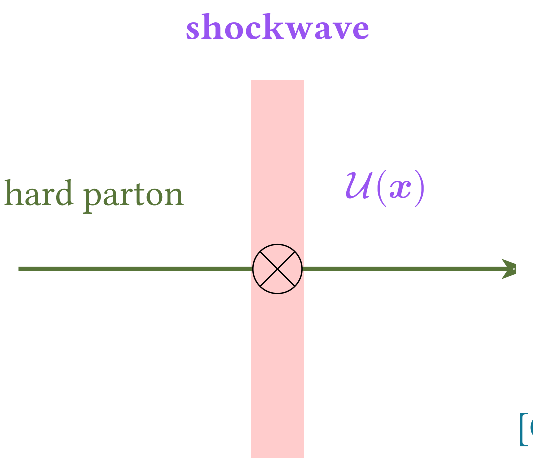

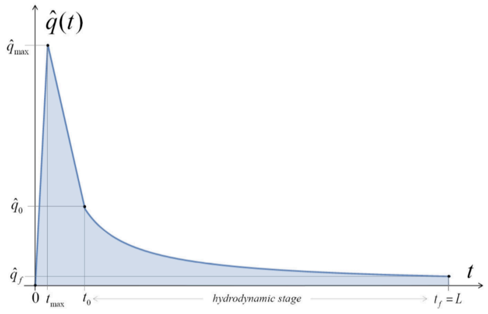

Figure 3: Schematic temporal evolution of $\hat{q}(t)$.

[Carrington et al. Phys. Lett. B 834, 137464 2022]

- Frozen background field during the short interaction.
- Interplay of Vacuum radiation and Shockwave insertion

[Balitsky Nucl. Phys. B 463, 99–160 1996; Kovchegov Phys. Rev. D 61, 74018 2000; Iancu & Venugopalan Quark-gluon plasma 4 249–3363 2003; Gelis & Jalilian-Marian Phys. Rev. D 66, 14021 2002]

LCPT

- In light-cone gauge $A^+ = 0$

$$
\begin{aligned}
S_F(x,y) &= \int \mathrm{d}q^- e^{i(x^+-y^+)\cdot q^-} \frac{\not{q}}{q^2+i\varepsilon} \\
&= \int \mathrm{d}q^- e^{i(x^+-y^+)\cdot q^-} \frac{1}{2q^+} \frac{q^+\gamma^- + \frac{\boldsymbol{q}^2}{2q^+}\gamma^+ + \boldsymbol{q}\cdot\boldsymbol{\gamma}}{q^- - \frac{\boldsymbol{q}}{2q^+} + i\varepsilon} + \frac{\gamma^+\left(q^- - \frac{\boldsymbol{q}^2}{2q^+}\right)}{2q^+\left(q^- - \frac{\boldsymbol{q}}{2q^+}\right)} \\
&= \theta(x^+-y^+)\frac{1}{2q^+}\frac{\bar{\not{q}}}{q^- - \frac{\boldsymbol{q}}{2q^+} + i\varepsilon} + \frac{\gamma^+}{2q^+}\delta(x^+-y^+) + \text{Reverse Order}
\end{aligned}
\tag{1}
$$

- Old-fashioned perturbation theory with x^+ time-ordering

[Brodsky et al. Phys. Rept. 301, 299–486 1998]

Quark Propagator

Eikonal propagation

$$S_{F(x,y)_{\beta\alpha}} =$$

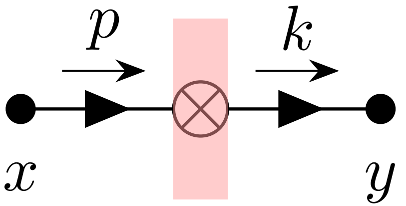

$$= \mathbf{1}_{\beta\alpha}\delta^{(2)}(\boldsymbol{x}-\boldsymbol{y})\delta(x^+-y^+)\,\mathrm{sign}(x^--y^-)\frac{\gamma^+}{4} + \int\frac{d^3p}{(2\pi)^3}\int\frac{d^3k}{(2\pi)^3} \tag{2}$$

$$\frac{\not{\overline{p}}\gamma^+\not{\overline{k}}}{4p^+k^+}(2\pi)\delta(p^+-k^+)e^{-ix\cdot\overline{p}+iy\cdot\overline{k}}\int d^2\boldsymbol{z}e^{-i\boldsymbol{z}\cdot(\boldsymbol{p}-\boldsymbol{k})}$$

$$\times\left\{\theta(k^+)\theta(x^+-y^+)\mathcal{U}_F(x^+,y^+;\boldsymbol{z})_{\beta\alpha}-\theta(-k^+)\theta(y^+-x^+)\mathcal{U}_F(y^+,x^+;\boldsymbol{z})_{\beta\alpha}\right\}.$$

[Balitsky Nucl. Phys. B 463, 99–160 1996; Kovchegov Phys. Rev. D 61, 74018 2000; Iancu & Venugopalan Quark-gluon plasma 4 249–3363 2003; Gelis & Jalilian-Marian Phys. Rev. D 66, 14021 2002; Gelis & Venugopalan Phys. Rev. D 69, 14019 2004; Fujii et al. Nucl. Phys. A 780, 146–174 2006]

Gluon Propagator

Adjoint representation

$$G^{\mu\nu}_{ab}(x,y) =$$

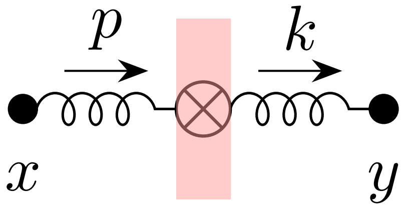

$$= G^{\mu\nu}_{ab,\ \mathrm{inst}}(x,y) + \int \frac{d^3p}{(2\pi)^3} \int \frac{d^3k}{(2\pi)^3} \frac{1}{2k^+} \sum_\lambda \varepsilon^\mu_\lambda(\overline{p}) \varepsilon^{*\nu}_\lambda\left(\overline{k}\right) \tag{3}$$

$$\times (2\pi)\delta(p^+ - k^+) e^{-ix\cdot\overline{p}+iy\cdot\overline{k}} \int d^2\boldsymbol{z} e^{-i\boldsymbol{z}\cdot(\boldsymbol{p}-\boldsymbol{k})}$$

$$\times \left\{\theta(k^+)\theta(x^+ - y^+)\mathcal{U}_A(x^+, y^+; \boldsymbol{z})_{ab} - \theta(-k^+)\theta(y^+ - x^+)\mathcal{U}_A(y^+, x^+; \boldsymbol{z})_{ab}\right\}.$$

[Balitsky Nucl. Phys. B 463, 99–160 1996; Kovchegov Phys. Rev. D 61, 74018 2000; Iancu & Venugopalan Quark-gluon plasma 4 249–3363 2003; Gelis & Jalilian-Marian Phys. Rev. D 66, 14021 2002; Gelis & Venugopalan Phys. Rev. D 69, 14019 2004; Fujii et al. Nucl. Phys. A 780, 146–174 2006]

Kinematics

- Incoming hard quark:

$$p_1 = (0^+, p_1^-, \mathbf{0}), \quad \ell = (\ell^+, \ell^-, \mathbf{0}) \tag{4}$$

- On-shell Outgoing pair:

$$p' = (p'^+, p'^-, \boldsymbol{p}'), \quad k' = (k'^+, k'^-, \boldsymbol{k}') \tag{5}$$

- Gluon momentum fraction

$$y = \frac{k'^+}{q'^+} = \frac{k'^+}{p'^+ + k'^+} \tag{6}$$

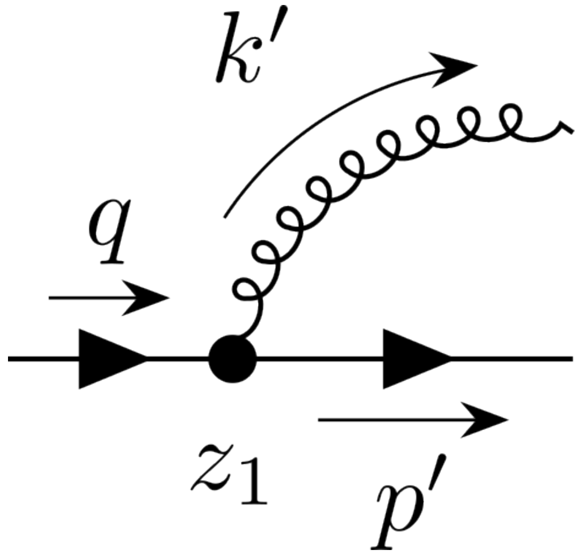

$\boldsymbol{b}$: quark position $\boldsymbol{r}$: gluon position $\boldsymbol{u} = \boldsymbol{r} - \boldsymbol{b}$: qg size

On-Shell Case

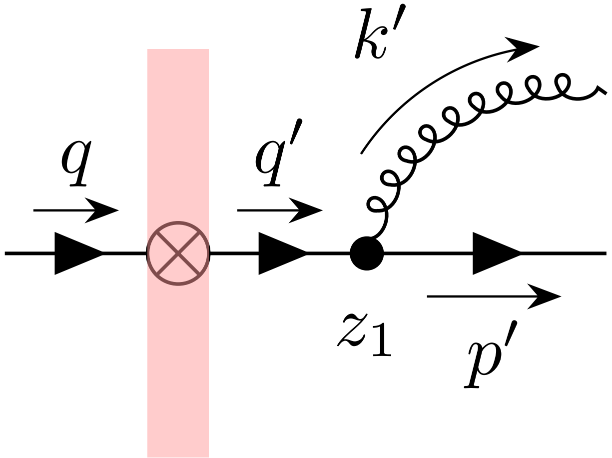

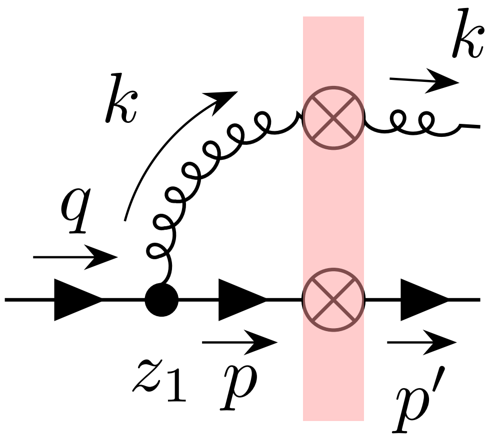

- **A**: Emission **after** the shockwave
- **B**: Emission **before** the shockwave

- On-shell parent $\longrightarrow$ two time orderings across the shockwave.

[Marquet Nucl. Phys. A 796, 41–60 2007]

Wave Function

- The $q \to qg$ wave function

$$\Psi^{q\to qg}(p', k') = $$

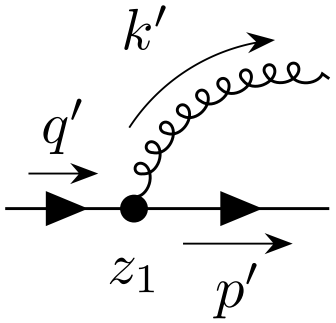

$$= \frac{\overline{u}(q'-k')\not{\varepsilon}^*_\lambda(k')u(q')}{(q'-k')^- - q'^- - k'^-} \tag{7}$$

- On-shell parent $\longrightarrow$ Energy denominator simply: $(\boldsymbol{k} - y\boldsymbol{q}')^{-2} \neq \infty$.
- Fourier Transform $\boldsymbol{q}' \to \boldsymbol{r} - \boldsymbol{b}$:

  $\longrightarrow$ Weizsäcker-Williams wave function:

$$\begin{aligned} \phi_0^\lambda(\boldsymbol{u}) &= \int d^2\boldsymbol{q}'\, e^{i\boldsymbol{u}\cdot\boldsymbol{q}'}\,\Psi^{q\to qg}(p', k') \\ &= 2i\sqrt{1-y}\frac{\boldsymbol{u}\cdot\varepsilon^*_\lambda}{2\pi\boldsymbol{u}^2}\left[\delta_{\lambda,s} + (1-y)\delta_{\lambda,-s}\right]. \end{aligned} \tag{8}$$

[Marquet Nucl. Phys. A 796, 41–60 2007]

Amplitude

After

$$\mathcal{A}_{\text{after}} =$$

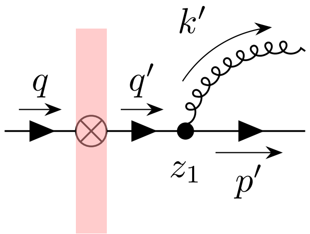

$$= -\mathcal{N}_0 \int d^2b d^2r e^{-i\boldsymbol{b}\cdot\boldsymbol{p}'} e^{-i\boldsymbol{r}\cdot\boldsymbol{k}'} \phi_0^\lambda(\boldsymbol{r}-\boldsymbol{b}) t^a \mathcal{U}_F(\boldsymbol{v})\,. \tag{9}$$

- Transverse center of mass

$\rightarrow$ $\boxed{\boldsymbol{v} = \boldsymbol{b} + y(\boldsymbol{r}-\boldsymbol{b}).}$

Before

$$\mathcal{A}_{\text{before}} =$$

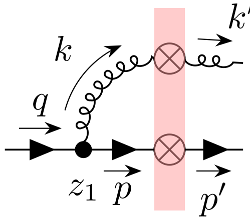

$$= \mathcal{N}_0 \int d^2b d^2r e^{-i\boldsymbol{b}\cdot\boldsymbol{p}'} e^{-i\boldsymbol{r}\cdot\boldsymbol{k}'} \phi_0^\lambda(\boldsymbol{r}-\boldsymbol{b}) t^b \mathcal{U}_F(\boldsymbol{b}) \mathcal{U}_A^{ba}(\boldsymbol{r})\,. \tag{10}$$

- Transverse positions:

$\rightarrow$ $\boxed{\boldsymbol{b}\text{: quark}}$

$\rightarrow$ $\boxed{\boldsymbol{r}\text{: gluon}}$

Total Amplitude

$$\mathcal{A}_{\text{on-shell}} = \mathcal{N}_0 \int d^2b\, d^2r\, e^{-i\delta \boldsymbol{r}\cdot(\boldsymbol{p}'+\boldsymbol{k}')} e^{-i\boldsymbol{R}\cdot\frac{\boldsymbol{k}'-\boldsymbol{p}'}{2}} \phi_0^\lambda(\delta\boldsymbol{r}) \left[\underbrace{t^b \mathcal{U}_F(\boldsymbol{b})\mathcal{U}_A(\boldsymbol{r})^{ba}}_{\text{After}} - \underbrace{t^a\mathcal{U}_F(\boldsymbol{v})}_{\text{Before}} \right]. \tag{11}$$

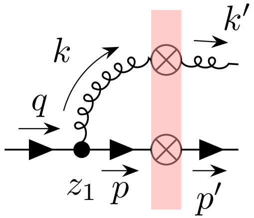

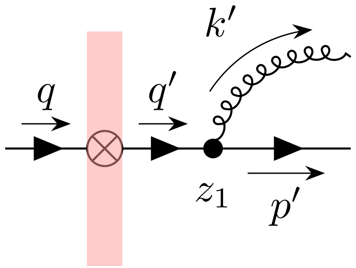

- Amplitude $\longrightarrow$ difference between **Before** and **After**.
- In vacuum: $\longrightarrow$ $\boxed{\mathcal{U} \to 1 \Rightarrow \mathcal{A} \to 0.}$

[Marquet Nucl. Phys. A 796, 41–60 2007]

Jets

- Jets emerge from the **splitting functions**

$$\mathcal{M}(\gamma^* q \to gq) = \mathcal{M}(\gamma^* q \to q) P_{qg}(y) \quad (12)$$

- Splitting function $P_{qg}(y)$ singular in IR
  $\longrightarrow$ IR divergences absorbed into **jet definition**

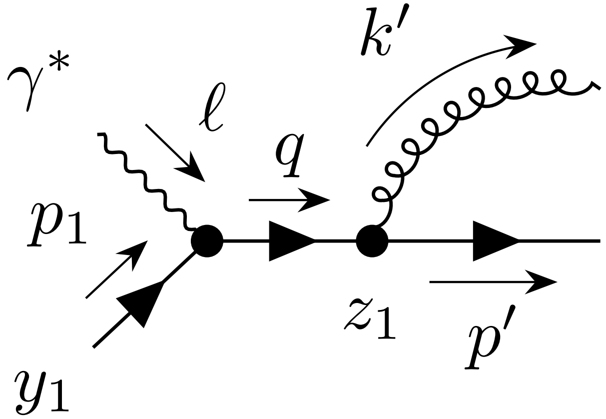

Jets

[Lappi & Paatelainen Annals Phys. 379, 34–66 2017]

- Je
- Sp

Setup

- DGLAP evolution: collinear divergence in cross section,
  UV renormalization in operator definition of PDF
- Starting point: bare nonsinglet quark distribution, UV divergent

$$f^0_{\text{n.s.}/h}(\mu, x) \equiv \frac{1}{4\pi x}\int \frac{\mathrm{d}^{D-2}\mathbf{k}}{(2\pi)^{D-2}} \frac{\langle h(p^+)|\, a^\dagger_q(xp^+,\mathbf{k})a_q(xp^+,\mathbf{k}) - a^\dagger_{\bar q}(xp^+,\mathbf{k})a_{\bar q}(xp^+,\mathbf{k})\,|h(p^+)\rangle}{\langle h(p^+)|h(p^+)\rangle}$$

- Take hadron = dressed quark with space-like $p^2 = -\mu_0^2 \implies$ **no IR divergences**

$$|h\rangle = \left|q(\mu_0^2)\right\rangle_{\text{int}} = \sqrt{Z_q(p^+)}\left[|q\rangle + \psi^{q\to qg}\,|qg\rangle + \psi^{q\to qgg}\,|qgg\rangle + \dots\right]$$

- At dim. reg scale $\mu = \mu_0$ off-shellness: no logs, identify DGLAP evolution from

$$f^0_{\text{n.s.}/q(\mu_0)}(\mu = \mu_0, x) = \delta(1-x) + \left(\frac{\alpha_s}{2\pi}\right)\frac{1}{\varepsilon}P^{-,(0)}(x) + \frac{1}{2}\left(\frac{\alpha_s}{2\pi}\right)^2\left[\frac{1}{\varepsilon}P^{-,(0)}\right]^2$$
$$+ \frac{1}{2}\left(\frac{\alpha_s}{2\pi}\right)^2\left[\frac{1}{\varepsilon}P^{-,(1)}(x)\right] + \text{finite, cross terms.}$$

Talk last week

21/25

Kinematics

- Incoming hard quark:

$$p_1 = (0^+, p_1^-, \mathbf{0}), \quad \ell = (\ell^+, \ell^-, \mathbf{0}) \tag{14}$$

- On-shell Outgoing pair:

$$p' = (p'^+, p'^-, \boldsymbol{p}'), \quad k' = (k'^+, k'^-, \boldsymbol{k}') \tag{15}$$

- Gluon momentum fraction

$$y = \frac{k'^+}{q'^+} = \frac{k'^+}{p'^+ + k'^+} \tag{16}$$

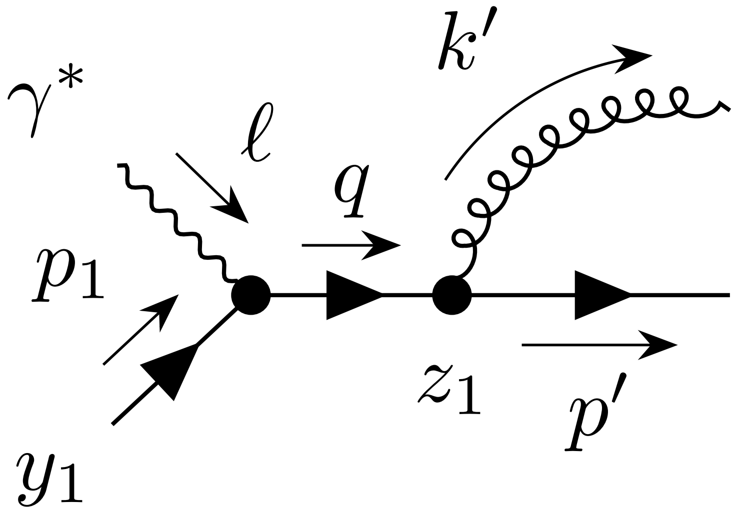

$\boldsymbol{b}$: quark position $\quad$ $\boldsymbol{r}$: gluon position $\quad$ $\boldsymbol{u} = \boldsymbol{r} - \boldsymbol{b}$: qg size

Off-shell Amplitude

- **A:** emission **after** the shockwave

  $$\boxed{y_1^+ < 0 < z_1^+}$$

- **B:** emission **before** the shockwave

  $$\boxed{y_1^+ < z_1^+ < 0}$$

- **C:** shockwave **before** the photon vertex

  $$\boxed{0 < y_1^+ < z_1^+}$$

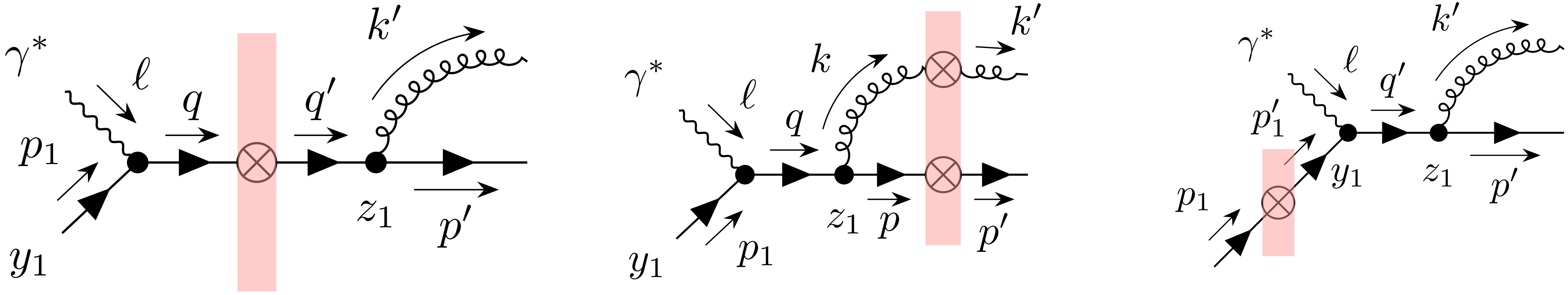

Vacuum radiation

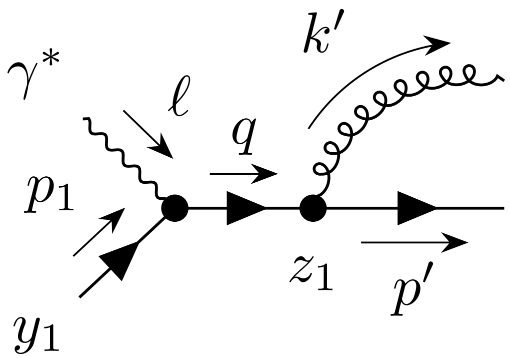

- Minus energy
  - z_1^+: $P^- = \bar{p}^- + \bar{k}^-$
  - y_1^+: $Q^- = p_1^- + \ell^-$

- **A:** $\boxed{y_1^+ < 0 < z_1^+}$

$$\int_{-\infty}^{0} dy_1^+ \int_{0}^{\infty} dz_1^+ \, \mathcal{V} = -\frac{1}{P^- - \bar{q}^- + i\varepsilon} \frac{1}{Q^- - \bar{q}^- + i\varepsilon}$$

- **B:** $\boxed{y_1^+ < z_1^+ < 0}$

$$\int_{-\infty}^{0} dy_1^+ \int_{y_1^+}^{0} dz_1^+ \, \mathcal{V} = \frac{1}{P^- - Q^- - i\varepsilon} \frac{1}{Q^- - \bar{q}^- + i\varepsilon}$$

- **C:** $\boxed{0 < y_1^+ < z_1^+}$

$$\int_{0}^{\infty} dy_1^+ \int_{y_1^+}^{\infty} dz_1^+ \, \mathcal{V} = \frac{1}{P^- - \bar{q}^- + i\varepsilon} \frac{1}{Q^- - P^- - i\varepsilon}$$

Energy Conservation

- The sum of the three time-orderings gives a delta function in minus energy

$$\begin{aligned}
&\frac{1}{\boldsymbol{P}^- - \bar{\boldsymbol{q}}^- + i\varepsilon}\frac{1}{\boldsymbol{Q}^- - \boldsymbol{P}^- - i\varepsilon} - \frac{1}{\boldsymbol{P}^- - \bar{\boldsymbol{q}}^- + i\varepsilon}\frac{1}{\boldsymbol{Q}^- - \bar{\boldsymbol{q}}^- + i\varepsilon} \\
&+\frac{1}{\boldsymbol{P}^- - \boldsymbol{Q}^- - i\varepsilon}\frac{1}{\boldsymbol{Q}^- - \bar{\boldsymbol{q}}^- + i\varepsilon} \\
&= \frac{1}{Q^- - \bar{q}^- + i\varepsilon}\left[\frac{1}{Q^- - P^- - i\varepsilon} - \frac{1}{Q^- - P^- + i\varepsilon}\right] \propto \frac{1}{Q^- - \bar{q}^- + i\varepsilon}\delta(Q^- - P^-)
\end{aligned} \tag{17}$$

Emission **After** Shockwave

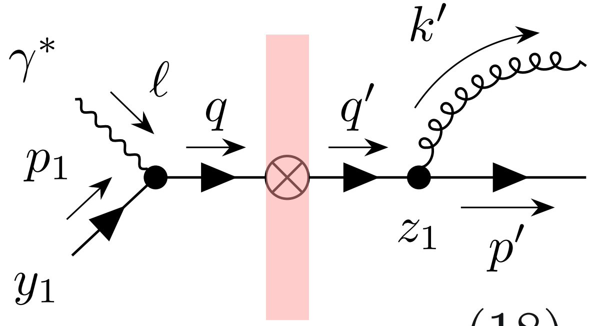

- Photon vertex:

$$\overline{u}(\overline{q})\not\varepsilon_\lambda(\ell)u(\overline{p}) = 2\sqrt{p_1^-\ell^+} \tag{18}$$

- Energy denominator ($\boldsymbol{q} = 0$):

$$p_1^- + \ell^- - \overline{p}^- - \overline{k}^- + i\varepsilon = -\frac{\boldsymbol{k}^2}{2\ell^+ y(1-y)} \tag{19}$$

- Weizsäcker-Williams wave function:

$$\phi_0^\lambda(\boldsymbol{u}) = 2i\sqrt{1-y}\frac{\boldsymbol{u}\cdot\boldsymbol{\varepsilon}_\lambda^*}{2\pi\boldsymbol{u}^2}\left[\delta_{\lambda,s} + (1-y)\delta_{\lambda,-s}\right] \tag{20}$$

Emission **After** Shockwave

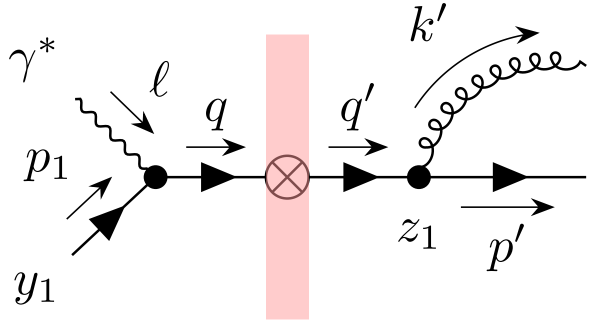

- Weizsäcker-Williams wave function:

$$\phi_0^\lambda(\boldsymbol{u}) = 2i\sqrt{1-y}\frac{\boldsymbol{u}\cdot\boldsymbol{\varepsilon}_\lambda^*}{2\pi\boldsymbol{u}^2}\left[\delta_{\lambda,s} + (1-y)\delta_{\lambda,-s}\right] \tag{21}$$

- Amplitude for ordering A:

$$\boxed{\mathcal{A}_A = -2eg\frac{\sqrt{p_1^-\ell^+}}{p_1^- + \ell^-}\int d^2b d^2r\, e^{-i\boldsymbol{b}\cdot\boldsymbol{p}'} e^{-i\boldsymbol{r}\cdot\boldsymbol{k}'}\phi_0^\lambda(\boldsymbol{u})t^a\mathcal{U}_F(\boldsymbol{v})_{\beta\alpha}\,. \tag{22}}$$

Emission **Before** Shockwave

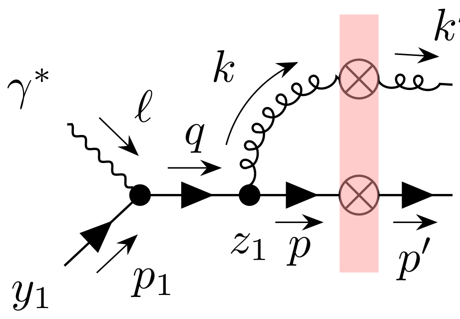

- Off-shell virtuality:

$$M^2 = y(1-y)\left(2\ell^+ p_1^- - Q^2\right)$$

- Energy denominator ($\boldsymbol{q} = 0$):

$$p_1^- + \ell^- - \overline{p}^- - \overline{k}^- + i\varepsilon = -\frac{\boldsymbol{k}^2 - M^2 - i\varepsilon}{2\ell^+ y(1-y)} \tag{23}$$

- $K_1\left(\sqrt{-M^2 - i\varepsilon}\right) \rightarrow i\varepsilon$ selects the side of **Branch cut**

$$K_1(ix) = \begin{cases} H^{(1)}(x) = -\frac{\pi}{2}[J_1(x) + iY_1(x)], & -\pi < \arg(x) < -\frac{\pi}{2} \\ H^{(2)}(x) = -\frac{\pi}{2}[J_1(x) - iY_1(x)], & -\frac{\pi}{2} < \arg(x) < \pi \end{cases} \tag{24}$$

Emission **Before** Shockwave

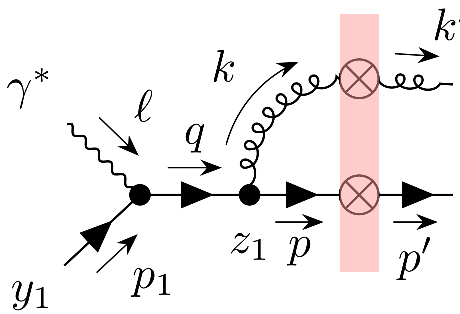

- $K_1\left(\sqrt{-M^2 - i\varepsilon}\right) \rightarrow i\varepsilon$ selects the side of **Branch cut**

$$K_1(ix) = \begin{cases} H^{(1)}(x) = -\frac{\pi}{2}[J_1(x) + iY_1(x)], & -\pi < \arg(x) < -\frac{\pi}{2} \\ H^{(2)}(x) = -\frac{\pi}{2}[J_1(x) - iY_1(x)], & -\frac{\pi}{2} < \arg(x) < \pi \end{cases} \tag{25}$$

- wave function:

$$\phi_-^\lambda(\boldsymbol{u}) = i\frac{(-iM)H^{(2)}(-iM\ |\boldsymbol{u}|)}{2\pi}\frac{\boldsymbol{u}\cdot\boldsymbol{\varepsilon}_\lambda^*}{|\boldsymbol{u}|}2\sqrt{1-y}\left[\delta_{\lambda,s} + (1-y)\delta_{\lambda,-s}\right] \tag{26}$$

- Amplitude:

$$\mathcal{A}_B = 2eg\frac{\sqrt{p_1^-\ell^+}}{p_1^- + \ell^-}\int d^2b d^2r e^{-i\boldsymbol{b}\cdot\boldsymbol{p}'}e^{-i\boldsymbol{r}\cdot\boldsymbol{k}'}\phi_-^\lambda(\boldsymbol{u})t^b\mathcal{U}_F(\boldsymbol{b})_{\beta\alpha}\mathcal{U}_A^{ba}(\boldsymbol{r})\,. \tag{27}$$

Shockwave **Before** Photon Vertex

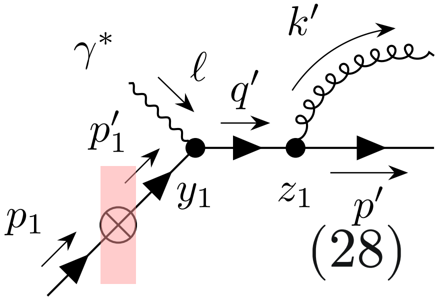

- Off-shell virtuality:

$$\sqrt{-M^2 + i\varepsilon} = iM \tag{28}$$

- Energy denominator prescription:

$$p_1^- + \ell^- - p'^- - k'^- - i\varepsilon = -\frac{\boldsymbol{k}'^2 - M^2 + i\varepsilon}{2\ell^+ y(1-y)} \tag{29}$$

- Amplitude contains both ϕ_+ and vacuum ϕ_0:

$$\frac{1}{p_1^- + \ell^- - p'^- - k'^- - i\varepsilon}\frac{\mathcal{N}}{2\ell^+} = -\int d^2\boldsymbol{r} e^{-i\boldsymbol{r}\cdot\boldsymbol{k}'}\left[\phi_+^\lambda(\boldsymbol{u}) - \phi_0^\lambda(\boldsymbol{u})\right] \tag{30}$$

Shockwave **Before** Photon Vertex

- Off-shell virtuality:

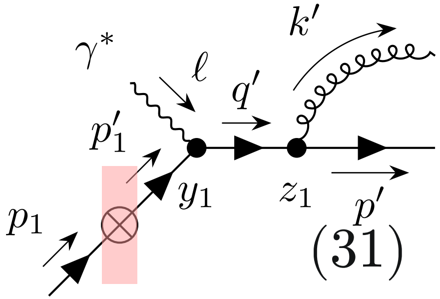

$$\sqrt{-M^2 + i\varepsilon} = iM \tag{31}$$

- Energy denominator prescription:

$$p_1^- + \ell^- - p'^- - k'^- - i\varepsilon = -\frac{\boldsymbol{k}'^2 - M^2 + i\varepsilon}{2\ell^+ y(1-y)} \tag{32}$$

- Amplitude for ordering C:

$$\mathcal{A}_C = 2eg\frac{\sqrt{p_1^- \ell^+}}{p_1^- + \ell^-}\int d^2b d^2r\, e^{-i\boldsymbol{b}\cdot\boldsymbol{p}'} e^{-i\boldsymbol{r}\cdot\boldsymbol{k}'}\left[\phi_0^\lambda(\boldsymbol{u}) - \phi_+^\lambda(\boldsymbol{u})\right] t^a \mathbf{1}_{\beta\alpha}\,. \tag{33}$$

Total Amplitude

- Use $\boldsymbol{u} = \boldsymbol{r} - \boldsymbol{b}$ and $\boldsymbol{v} = \boldsymbol{b} + y(\boldsymbol{r} - \boldsymbol{b})$:

$$\boldsymbol{b} = \boldsymbol{v} - y\boldsymbol{u}, \qquad \boldsymbol{r} = \boldsymbol{v} + (1-y)\boldsymbol{u}, \tag{34}$$

- Total amplitude:

$$\mathcal{A}_{\text{total}} = 2eg\frac{\sqrt{p_1^- \ell^+}}{p_1^- + \ell^-} \int d^2\boldsymbol{u} d^2\boldsymbol{v}\, e^{-i\boldsymbol{v}\cdot(\boldsymbol{p}'+\boldsymbol{k}')} e^{-i\boldsymbol{u}\cdot((1-y)\boldsymbol{k}'-y\boldsymbol{p}')} \tag{35}$$

$$\times \Big[\underbrace{\phi_-^\lambda(\boldsymbol{u}) t^b \mathcal{U}_F(\boldsymbol{b})_{\beta\alpha} \mathcal{U}_A(\boldsymbol{r})^{ba}}_{\mathbf{B}} - \underbrace{\phi_0^\lambda(\boldsymbol{u}) t^a \mathcal{U}_F(\boldsymbol{v})_{\beta\alpha}}_{\mathbf{A}} + \underbrace{[\phi_0^\lambda(\boldsymbol{u}) - \phi_+^\lambda(\boldsymbol{u})] t^a \mathbf{1}_{\beta\alpha}}_{\mathbf{C}} \Big]$$

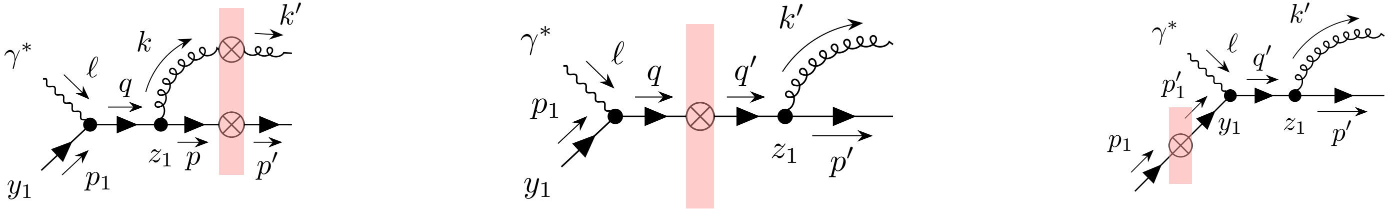

Vacuum Limit

- Taking $\mathcal{U}_{F/A} \to \mathbf{1}$:

$$\mathcal{A}_{\text{total}} = 2eg\frac{\sqrt{p_1^- \ell^+}}{p_1^- + \ell^-} \int d^2\boldsymbol{u} d^2\boldsymbol{v}\, e^{-i\boldsymbol{v}\cdot(\boldsymbol{p}'+\boldsymbol{k}')} e^{-i\boldsymbol{u}\cdot((1-y)\boldsymbol{k}'-y\boldsymbol{p}')} t^a \left[\phi_-^\lambda(\boldsymbol{u}) - \phi_+^\lambda(\boldsymbol{u})\right]. \quad (36)$$

$\longrightarrow$ On-shell contribution $\#\phi_0 \to 0$.

- Integral $\int d\boldsymbol{v} \longrightarrow (2\pi)^2\delta^{(2)}(\boldsymbol{p}' + \boldsymbol{k}')$, transverse momentum conservation.
- Difference $\phi_-^\lambda - \phi_+^\lambda \longrightarrow$ minus-momentum conservation

$$\phi_-^\lambda - \phi_+^\lambda = -\phi_J^\lambda(\boldsymbol{u})$$

$$\text{Momentum space} \Rightarrow \quad \frac{1}{\boldsymbol{k}^2 - M^2 - i\varepsilon} - \frac{1}{\boldsymbol{k}^2 - M^2 + i\varepsilon} = 2\pi i\delta(\boldsymbol{k}^2 - M^2) \quad (37)$$

Vacuum Subtraction

- The vacuum square contains the usual square of an S-matrix delta function:

$$\int d^2\boldsymbol{u} d^2\overline{\boldsymbol{u}} e^{-i\boldsymbol{l}\cdot\boldsymbol{u}} e^{i\boldsymbol{l}\cdot\overline{\boldsymbol{u}}} \phi_J^\lambda(\boldsymbol{u}) \phi_J^{\lambda *}(\overline{\boldsymbol{u}}) \propto \left[\boldsymbol{\delta(l^2 - M^2)}\right]^{\boldsymbol{2}} \tag{38}$$

- Organize the finite medium-dependent object as

$$\boxed{\langle|\mathcal{A}|^2\rangle - |\mathcal{A}_{\text{vac}}|^2 = \langle|\mathcal{A}_{\text{med}}|^2\rangle + 2\,\text{Re}\langle\mathcal{A}_{\text{vac}}\mathcal{A}_{\text{med}}^\dagger\rangle, \quad \mathcal{A}_{\text{med}} = \mathcal{A} - \mathcal{A}_{\text{vac}}.} \tag{39}$$

Medium Average

- Dipole and multipole correlators:

$$
\begin{aligned}
S^2_{q\bar{q}}(\boldsymbol{v},\overline{\boldsymbol{v}}) &= \frac{1}{N_c}\langle \mathrm{Tr}\left[\mathcal{U}_{F(\boldsymbol{v})}\mathcal{U}_F^{\dagger(\overline{\boldsymbol{v}})}\right]\rangle \\
S^3_{qg\bar{q}}(\boldsymbol{b},\boldsymbol{r},\overline{\boldsymbol{v}}) &= \frac{1}{C_F N_c}\langle \mathrm{Tr}\left[t^b\mathcal{U}_{F(\boldsymbol{b})}t^a\mathcal{U}_F^{\dagger(\overline{\boldsymbol{v}})}\right]\mathcal{U}^{ba}_{A(\boldsymbol{r})}\rangle \\
S^4_{qg\bar{q}g}\left(\boldsymbol{b},\overline{\boldsymbol{b}},\boldsymbol{r},\overline{\boldsymbol{r}}\right) &= \frac{1}{C_F N_c}\langle \mathrm{Tr}\left[\mathcal{U}_{F(\boldsymbol{b})}\mathcal{U}_F^{\dagger\left(\overline{\boldsymbol{b}}\right)}t^a t^b\right]\mathcal{U}^{ac}_{A(\boldsymbol{r})}\mathcal{U}_A^{\dagger(\overline{\boldsymbol{r}})^{cb}}\rangle
\end{aligned}
\tag{40}
$$

Square of the Amplitude

$$\langle|\mathcal{A}_{\text{med}}|^2\rangle = 4e^2g^2C_FN_c\frac{p_1^-\ell^+}{(p_1^-+\ell^-)^2}\int d^2\boldsymbol{v}d^2\overline{\boldsymbol{v}}d^2\boldsymbol{u}d^2\overline{\boldsymbol{u}}e^{-i(\boldsymbol{v}-\overline{\boldsymbol{v}})\cdot(\boldsymbol{p}'+\boldsymbol{k}')}e^{-i(\boldsymbol{u}-\overline{\boldsymbol{u}})\cdot((1-y)\boldsymbol{k}'-y\boldsymbol{p}')}$$
$$\times\left\{\boldsymbol{\phi_0^\lambda(u)\phi_0^{\lambda*}(\overline{u})\left[S^4(b,\overline{b},r,\overline{r})-S^3(b,r,\overline{v})-S^3\left(\overline{b},\overline{r},v\right)+S^2(v,\overline{v})\right]}\right. \tag{41}$$

Square of the Amplitude

$$\begin{aligned}\langle|\mathcal{A}_{\text{med}}|^2\rangle = 4e^2g^2C_FN_c\frac{p_1^-\ell^+}{(p_1^-+\ell^-)^2}\int d^2\boldsymbol{v}d^2\overline{\boldsymbol{v}}d^2\boldsymbol{u}d^2\overline{\boldsymbol{u}}e^{-i(\boldsymbol{v}-\overline{\boldsymbol{v}})\cdot(\boldsymbol{p}'+\boldsymbol{k}')}e^{-i(\boldsymbol{u}-\overline{\boldsymbol{u}})\cdot((1-y)\boldsymbol{k}'-y\boldsymbol{p}')}\\ \times\Big\{\phi_0^\lambda(u)\phi_0^{\lambda*}(\overline{u})\big[S^4(\boldsymbol{b},\overline{\boldsymbol{b}},\boldsymbol{r},\overline{\boldsymbol{r}})-S^3(\boldsymbol{b},\boldsymbol{r},\overline{\boldsymbol{v}})-S^3(\overline{\boldsymbol{b}},\overline{\boldsymbol{r}},\boldsymbol{v})+S^2(\boldsymbol{v},\overline{\boldsymbol{v}})\big]\\ +\big[\phi_-^\lambda(u)-\phi_0^\lambda(u)\big]\phi_0^{\lambda*}(\overline{\boldsymbol{u}})\Big[S^4\Big(\boldsymbol{b},\overline{\boldsymbol{b}},\boldsymbol{r},\overline{\boldsymbol{r}}\Big)-S^3(\boldsymbol{b},\boldsymbol{r},\overline{\boldsymbol{v}})\Big]\\ +\phi_0^\lambda(\boldsymbol{u})\big[\phi_-^{\lambda*}(\overline{u})-\phi_0^{\lambda*}(\overline{u})\big]\Big[S^4\Big(\boldsymbol{b},\overline{\boldsymbol{b}},\boldsymbol{r},\overline{\boldsymbol{r}}\Big)-S^3\Big(\overline{\boldsymbol{b}},\overline{\boldsymbol{r}},\boldsymbol{v}\Big)\Big]\\ +\big[\phi_-^\lambda(u)-\phi_0^\lambda(u)\big]\big[\phi_-^{\lambda*}(\overline{u})-\phi_0^{\lambda*}(\overline{u})\big]\Big[S^4\Big(\boldsymbol{b},\overline{\boldsymbol{b}},\boldsymbol{r},\overline{\boldsymbol{r}}\Big)+1\Big]\Big\}.\end{aligned} \tag{42}$$

Square of the Amplitude

$$\langle|\mathcal{A}_{\text{med}}|^2\rangle = 4e^2g^2C_FN_c\frac{p_1^-\ell^+}{(p_1^-+\ell^-)^2}\int d^2\boldsymbol{v}d^2\overline{\boldsymbol{v}}d^2\boldsymbol{u}d^2\overline{\boldsymbol{u}}e^{-i(\boldsymbol{v}-\overline{\boldsymbol{v}})\cdot(\boldsymbol{p}'+\boldsymbol{k}')}e^{-i(\boldsymbol{u}-\overline{\boldsymbol{u}})\cdot((1-y)\boldsymbol{k}'-y\boldsymbol{p}')}$$
$$\times\Big\{\phi_0^\lambda(\boldsymbol{u})\phi_0^{\lambda*}(\overline{\boldsymbol{u}})\big[S^4(\boldsymbol{b},\overline{\boldsymbol{b}},\boldsymbol{r},\overline{\boldsymbol{r}})-S^3(\boldsymbol{b},\boldsymbol{r},\overline{\boldsymbol{v}})-S^3(\overline{\boldsymbol{b}},\overline{\boldsymbol{r}},\boldsymbol{v})+S^2(\boldsymbol{v},\overline{\boldsymbol{v}})\big]$$
$$+\big[\phi_-^\lambda(\boldsymbol{u})-\phi_0^\lambda(\boldsymbol{u})\big]\phi_0^{\lambda*}(\overline{\boldsymbol{u}})\Big[S^4\Big(\boldsymbol{b},\overline{\boldsymbol{b}},\boldsymbol{r},\overline{\boldsymbol{r}}\Big)-S^3(\boldsymbol{b},\boldsymbol{r},\overline{\boldsymbol{v}})\Big] \tag{43}$$
$$+\phi_0^\lambda(\boldsymbol{u})\big[\phi_-^{\lambda*}(\overline{\boldsymbol{u}})-\phi_0^{\lambda*}(\overline{\boldsymbol{u}})\big]\Big[S^4\Big(\boldsymbol{b},\overline{\boldsymbol{b}},\boldsymbol{r},\overline{\boldsymbol{r}}\Big)-S^3\Big(\overline{\boldsymbol{b}},\overline{\boldsymbol{r}},\boldsymbol{v}\Big)\Big]$$
$$+\big[\phi_-^\lambda(\boldsymbol{u})-\phi_0^\lambda(\boldsymbol{u})\big]\big[\phi_-^{\lambda*}(\overline{\boldsymbol{u}})-\phi_0^{\lambda*}(\overline{\boldsymbol{u}})\big]\Big[S^4\Big(\boldsymbol{b},\overline{\boldsymbol{b}},\boldsymbol{r},\overline{\boldsymbol{r}}\Big)+1\Big]\Big\}.$$

- Setting $M\to 0$ gives $\big[\phi_-^\lambda(\boldsymbol{u})-\phi_0^\lambda(\boldsymbol{u})\big]\to 0$
  - $\longrightarrow$ recovering [Marquet Nucl. Phys. A 796, 41–60 2007]

Relevant Scales

- The wave function

$$\phi_-^\lambda(\boldsymbol{u}) \propto M[J_1(M\ |u|) - iY_1(M\ |u|)]\frac{\boldsymbol{u}\cdot\boldsymbol{\varepsilon}_\lambda^*}{|u|}, \tag{44}$$

  $\longrightarrow$ Selects transverse size $u \approx 1/M$.
- Dipole correlator

$$S(u) \approx \exp\left(-Q_s^2\frac{u^2}{4}\right). \tag{45}$$

  $\longrightarrow$ Resolves transverse sizes $u \approx 1/Q_s$.

Small Virtuality $M^2 \ll Q_s^2$

- Dipole correlators sets transverse size

$$u \approx 1/Q_s \quad \Rightarrow \quad Mu \ll 1. \tag{46}$$

- Small-M $|u|$ expansion:

$$J_1(M|u|) \approx 0, \quad Y_1(M|u|) \approx -\frac{2}{\pi M|u|}, \quad \Rightarrow \quad \phi_-^\lambda(\boldsymbol{u}) = \phi_0^\lambda(\boldsymbol{u})\,. \tag{47}$$

The square matrix element reduces to the on-shell case.

$$\phi_0^\lambda(\boldsymbol{u})\phi_0^{\lambda *}(\overline{\boldsymbol{u}})\left[S^4(\boldsymbol{b},\overline{\boldsymbol{b}},\boldsymbol{r},\overline{\boldsymbol{r}}) - S^3(\boldsymbol{b},\boldsymbol{r},\overline{\boldsymbol{v}}) - S^3\left(\overline{\boldsymbol{b}},\overline{\boldsymbol{r}},\boldsymbol{v}\right) + S^2(\boldsymbol{v},\overline{\boldsymbol{v}})\right] \tag{48}$$

High Virtuality $M^2 \gg Q_s^2$

- Large-Mu Hankel phase:

$$H_1^{(2)}(M|u|) \sim \frac{e^{-iM|u|}}{\sqrt{M|u|}}, \quad M \gg Q_s \quad \Rightarrow \quad u \approx 1/M \ll 1/Q_s. \tag{49}$$

- Small dipole:

$$S(u) = \exp\left(-Q_s^2 \frac{u^2}{4}\right) \approx 1 - Q_s^2 \frac{u^2}{4}, \quad 1 - S(u) \approx Q_s^2/(4M^2). \tag{50}$$

- Medium correction:

$$\frac{|\mathcal{A}_{\text{med}}|^2}{|\mathcal{A}_{\text{vac}}|^2} \approx \mathcal{O}\left(\frac{Q_s^2}{M^2}\right). \tag{51}$$

- Vacuum-like radiation dominates;
  $\longrightarrow$ Suppressed medium corrections.

Intermediate Virtuality $M^2 \approx Q_s^2$

- Two transverse scales

$$u \approx 1/Q_s \approx 1/M, \quad Mu \approx 1. \tag{52}$$

- Important contributions from all terms

$$\begin{aligned}
&\boldsymbol{\phi_0^\lambda(u)\phi_0^{\lambda*}(\overline{u})\left[S^4(b,\overline{b},r,\overline{r}) - S^3(b,r,\overline{v}) - S^3(\overline{b},\overline{r},v) + S^2(v,\overline{v})\right]} \\
&+\left[\boldsymbol{\phi_-^\lambda(u) - \phi_0^\lambda(u)}\right]\phi_0^{\lambda*}(\overline{\boldsymbol{u}})\left[S^4\left(\boldsymbol{b},\overline{\boldsymbol{b}},\boldsymbol{r},\overline{\boldsymbol{r}}\right) - S^3(\boldsymbol{b},\boldsymbol{r},\overline{\boldsymbol{v}})\right] \\
&+\phi_0^\lambda(\boldsymbol{u})\left[\boldsymbol{\phi_-^{\lambda*}(\overline{u}) - \phi_0^{\lambda*}(\overline{u})}\right]\left[S^4\left(\boldsymbol{b},\overline{\boldsymbol{b}},\boldsymbol{r},\overline{\boldsymbol{r}}\right) - S^3\left(\overline{\boldsymbol{b}},\overline{\boldsymbol{r}},\boldsymbol{v}\right)\right] \\
&+\left[\boldsymbol{\phi_-^\lambda(u) - \phi_0^\lambda(u)}\right]\left[\boldsymbol{\phi_-^{\lambda*}(\overline{u}) - \phi_0^{\lambda*}(\overline{u})}\right]\left[S^4\left(\boldsymbol{b},\overline{\boldsymbol{b}},\boldsymbol{r},\overline{\boldsymbol{r}}\right) + 1\right].
\end{aligned} \tag{53}$$

- Interplay between Glasma scales and virtuality.

Conclusions

Takeaways

- Off-shell radiation introduces a new hard scale M^2 in the shockwave calculation.
- The glasma resolves transverse sizes $u \approx 1/Q_s$:

$$M^2 \ll Q_s^2 \quad \Rightarrow \quad \text{on-shell limit}, \quad M^2 \gg Q_s^2 \quad \Rightarrow \quad \text{color transparency}. \tag{54}$$

- The glasma selects part of early shower with virtuality of order $\sim Q_s^2$.

Outlook

- Compute the medium-induced spectrum $\frac{\mathrm{d}N}{\mathrm{d}y d^2\boldsymbol{k}'}$ and compare to on-shell results.
- Understand interference term $2\,\mathrm{Re}\langle \mathcal{A}_{\mathrm{vac}} \mathcal{A}_{\mathrm{med}}^{\dagger} \rangle$.

Bibliography

[1] S. Chatrchyan and others, "Observation of Long-Range Near-Side Angular Correlations in Proton-Lead Collisions at the LHC," *Phys. Lett. B*, vol. 718, pp. 795–814, 2013, doi: 10.1016/j.physletb.2012.11.025.

[2] S. Chatrchyan and others, "Multiplicity and Transverse Momentum Dependence of Two- and Four-Particle Correlations in pPb and PbPb Collisions," *Phys. Lett. B*, vol. 724, pp. 213–240, 2013, doi: 10.1016/j.physletb.2013.06.028.

[3] V. Khachatryan and others, "Evidence for collectivity in pp collisions at the LHC," *Phys. Lett. B*, vol. 765, pp. 193–220, 2017, doi: 10.1016/j.physletb.2016.12.009.

[4] A. Hayrapetyan and others, "Observation of Suppressed Charged-Particle Production in Ultrarelativistic Oxygen-Oxygen Collisions," *Phys. Rev. Lett.*, vol. 136, no. 16, p. 162301, 2026, doi: 10.1103/89sf-9t1x.

[5] M. E. Carrington, A. Czajka, and S. Mrowczynski, "Jet quenching in glasma," *Phys. Lett. B*, vol. 834, p. 137464, 2022, doi: 10.1016/j.physletb.2022.137464.

[6] D. Avramescu, V. Băran, V. Greco, A. Ipp, D. I. Müller, and M. Ruggieri, "Simulating jets and heavy quarks in the glasma using the colored particle-in-cell method," *Phys. Rev. D*, vol. 107, no. 11, p. 114021, 2023, doi: 10.1103/PhysRevD.107.114021.

[7] A. Ipp, D. I. Müller, and D. Schuh, "Jet momentum broadening in the pre-equilibrium Glasma," *Phys. Lett. B*, vol. 810, p. 135810, 2020, doi: 10.1016/j.physletb.2020.135810.

[8] R. Baier, Y. L. Dokshitzer, A. H. Mueller, S. Peigne, and D. Schiff, "Radiative energy loss of high-energy quarks and gluons in a finite volume quark - gluon plasma," *Nucl. Phys. B*, vol. 483, pp. 291–320, 1997, doi: 10.1016/S0550-3213(96)00553-6.

[9] I. Balitsky, "Operator expansion for high-energy scattering," *Nucl. Phys. B*, vol. 463, pp. 99–160, 1996, doi: 10.1016/0550-3213(95)00638-9.

[10] Y. V. Kovchegov, "Unitarization of the BFKL pomeron on a nucleus," *Phys. Rev. D*, vol. 61, p. 74018, 2000, doi: 10.1103/PhysRevD.61.074018.

[11] E. Iancu and R. Venugopalan, "The Color glass condensate and high-energy scattering in QCD," in *Quark-gluon plasma 4*, R. C. Hwa and X.-N. Wang, Eds., 2003, pp. 249–3363. doi: 10.1142/9789812795533_0005.

[12] F. Gelis and J. Jalilian-Marian, "Photon production in high-energy proton nucleus collisions," *Phys. Rev. D*, vol. 66, p. 14021, 2002, doi: 10.1103/PhysRevD.66.014021.

Bibliography

[13] S. J. Brodsky, H.-C. Pauli, and S. S. Pinsky, "Quantum chromodynamics and other field theories on the light cone," *Phys. Rept.*, vol. 301, pp. 299–486, 1998, doi: 10.1016/S0370-1573(97)00089-6.

[14] F. Gelis and R. Venugopalan, "Large mass q anti-q production from the color glass condensate," *Phys. Rev. D*, vol. 69, p. 14019, 2004, doi: 10.1103/PhysRevD.69.014019.

[15] H. Fujii, F. Gelis, and R. Venugopalan, "Quark pair production in high energy pA collisions: General features," *Nucl. Phys. A*, vol. 780, pp. 146–174, 2006, doi: 10.1016/j.nuclphysa.2006.09.012.

[16] C. Marquet, "Forward inclusive dijet production and azimuthal correlations in p(A) collisions," *Nucl. Phys. A*, vol. 796, pp. 41–60, 2007, doi: 10.1016/j.nuclphysa.2007.09.001.

[17] T. Lappi and R. Paatelainen, "The one loop gluon emission light cone wave function," *Annals Phys.*, vol. 379, pp. 34–66, 2017, doi: 10.1016/j.aop.2017.02.002.

Backup

Wave Functions

- Momentum-space relation to the vacuum wave function:

$$\phi_0^\lambda(\boldsymbol{k}) = 2\sqrt{1-y}\left[\delta_{\lambda,s} + (1-y)\delta_{\lambda,-s}\right]\frac{\boldsymbol{k}\cdot\varepsilon_\lambda^*}{\boldsymbol{k}^2}$$
$$\phi_-^\lambda(\boldsymbol{k}) = \frac{\boldsymbol{k}^2}{\boldsymbol{k}^2 - M^2 - i\varepsilon}\phi_0^\lambda(\boldsymbol{k}) \tag{55}$$
$$\phi_+^\lambda(\boldsymbol{k}) = \frac{\boldsymbol{k}^2}{\boldsymbol{k}^2 - M^2 + i\varepsilon}\phi_0^\lambda(\boldsymbol{k})$$

- Coordinate-space

$$\phi_-^\lambda(\boldsymbol{u}) = \phi_Y^\lambda(\boldsymbol{u}) - \frac{1}{2}\phi_J^\lambda(\boldsymbol{u}), \phi_+^\lambda(\boldsymbol{u}) = \phi_Y^\lambda(\boldsymbol{u}) + \frac{1}{2}\phi_J^\lambda(\boldsymbol{u}) \tag{56}$$

Wave Functions

$\phi_Y^\lambda \to \phi_0^\lambda$ as $M^2 \to 0$, while ϕ_J^λ is the on-shell discontinuity.